

An Ecological Robustness-Oriented Approach for Power System Network Expansion

Hao Huang^{a,*}, Zeyu Mao^a, Varuneswara Panyam^{b,1}, Astrid Layton^b, Katherine Davis^a

^aDepartment of Electrical and Computer Engineering, Texas A&M University, College Station, TX, USA

^bJ. Mike Walker '66 Department of Mechanical Engineering, Texas A&M University, College Station, TX, USA

Abstract

Electric power grids are critical infrastructure that support modern society by supplying electric energy to critical infrastructure systems. Incidents are increasing that range from natural disasters to cyber attacks. These incidents threaten the reliability of power systems and create disturbances that affect the whole society. While existing standards and technologies are being applied to proactively improve power system reliability and resilience, there are still widespread electricity outages that cause billions of dollars in economic loss annually and threaten societal function and safety. Improving resilience in preparation for such events warrants strategic network design to harden the system. This paper presents an approach to strengthen power system security and reliability against disturbances by expanding the network structure from an ecosystems perspective.

Ecosystems have survived a wide range of disturbances over a long time period, and an ecosystem's robust structure has been identified as the key element for its survivability. In this paper, we first present a study of the correlation of ecological robustness and power system structures. Then, we present a mixed-integer nonlinear programming problem (MINLP) that expands the transmission network structure to maximize ecological robustness with power system constraints for an improved ability to absorb disturbances. We solve the MINLP problem for the IEEE 24 Bus Reliability Test System and three synthetic power grids with 200-, 500- and 2000-buses, respectively. Our evaluation results show the optimized power systems have increased the network's robustness, more equally distributed power flows, and less violations under different levels of contingencies.

Keywords: Power Networks Design; Ecological Robustness; Mixed-Integer Nonlinear Programming; Network Optimization; Power System Reliability; Power System Resilience

1. Introduction

Power grids deliver the electric energy that ensures the functionality of modern society. This reliance requires modern power grids to be reliable and secure, but an aging infrastructure and continually increasing demands make the existing network more vulnerable to physical disturbances and natural disasters [1, 2, 3]. The integration of communication networks into critical infrastructure further increases the risk of cyber-originated and combined cyber-physical attacks, which can cause unexpected power outages [4, 5]. It is essential to improve a power system's inherent abilities of preparing for, ensuring and recovering from extreme

events. Constructing *resilient* grid networks lays the foundation for such inherent abilities.

Resilience is a property of systems that describes their ability to operate during and recover from adverse situations to resume normal operations. Resilience depends on the system's elements, their configuration and interactions, and the surrounding environment [6]. From a regional transmission operator perspective, Chen *et al.* emphasize the necessity of constructing a robust grid to allow operators to address various contingencies on any given day [7]. In [8], Moreno *et al.* point out that modern power grids need to incorporate resilience against extreme events into the network planning process. In [9], Gholami *et al.* list different areas of resilience enhancement regarding system planning and operations, where the planning (long-term) resilience enhancements lay the foundation for operational (short-term) resilience enhancements, and oper-

*Corresponding author, email: hao.huang@tamu.edu

¹Currently working at Ceva Sante Animale, Lenexa, KS

ational (short-term) resilience enhancements guide the planning strategies (long-term). These works highlight the importance of network construction for enhancing power system resilience against adversaries, while motivating the need to better understand and characterize how to utilize network design effectively against extreme events.

There are various frameworks and metrics that have been proposed to capture a power system’s resilience that consider the system’s operation status, network structure, equipment, and hazards. Several works also consider design-based system approaches. For example, in [10], Ouyang and Duenas-Osorio present a probabilistic modeling approach to quantify power system resilience under a hurricane. Different approaches were analyzed for their ability to improve power system resilience and reduce economic loss, finding that organizational resilience *can* improve both goals. Prior work has also pointed out that redundant and robust network structures are effective for improving power system resilience under extreme conditions [11, 12]. A series of resilience metrics, based on a multi-phase resilience trapezoid for power system operational and infrastructure resilience [11], and sequential Monte-Carlo-based time-series simulation models to assess power system resilience [12], have been used. An alternate availability-based engineering resilience metric using a dynamic Bayesian network evaluation methodology was used to emphasize the importance of component redundancy in increasing power system resilience [13]. These works all support the ability to construct a robust and redundant power grid network such that the system’s ability to absorb disturbances is improved and the power supply is ensured during disturbances. These works proactively quantify power system resilience under various contingencies and suggest specific enhancement methods for particular elements, such as to add redundant protection devices for critical assets or to construct redundant branches for the vulnerable ones, but they do not provide a quantitative guideline to design a *robust* and *redundant* power grid network to enhance its inherent ability of absorbing disturbances.

A promising system design approach for improving grid resilience uses inspiration from ecosystems to translate their survivability traits to power grids. Ecosystems have evolved over millions of years to survive disturbances. This long-term work to model and understand these characteristics of ecosystems results in a potentially novel benchmark for robust, sustainable, and efficient networks design. Prior work has shown that the resilience of ecosystems can successfully be translated to water distribution networks [14],

supply chains [15, 16], industrial by-product networks [17], and more general large scale systems of systems [18, 19]. Previous work by the authors has also applied ecological robustness to power system network design. The work was able to use network topology with power flow information, observing an improvement of power system robustness and reliability [20, 21]. The approach uses the quantitative graph theory-based metric ecological robustness [22, 23] as an optimization goal for steady state directional graph representations of the human networks.

In [20, 21], the optimization model focuses on the network structure without explicitly including power system constraints, such as the power balance equations and operating limits. Thus, the optimization process searches the whole domain for the optimal solution and only checks power system feasibility post-optimization, which reduces its efficiency, making it only solvable with small cases. The optimization model in [20, 21] is based on a common power system approximation called the Direct Current (DC) power flow, which does not consider power losses, bus voltage, and reactive power support. While the DC power flow is a simple and often useful mechanism to estimate real power flows, the optimized network structure found using this approximation may be suboptimal for power system operation which is best represented with the full Alternating Current (AC) power flow equations.

Ecological robustness has further been improved in grid studies while considering power system constraints by modeling the problem as a mixed-integer nonlinear programming (MINLP) problem that solves for a bio-inspired robust power network design [24]. A binary decision variable was introduced for candidate branches, so that the ecological robustness was dependent on binary decision variables as well as the power flow distribution. The optimal ecological robustness decided the construction of candidate branches and the power flow distribution. The proposed MINLP problem was built with the transmission network expansion (TNEP) model in `PowerModels.jl` [25]. However, the formulation of ecological robustness associates with logarithm functions, which requires the entries’ domain to be positive. With the integration of power flow models, the MINLP problem in [24] is a non-convex, nonlinear problem. Thus, the previous MINLP was unable to guarantee feasible solutions for large power system cases.

This paper relaxes the formulation of ecological robustness with a Taylor Series Expansion for the logarithm functions to ensure the validity of the proposed optimization model. It also proposes an algorithm to limit the searching domain, which improves the solv-

ability and efficiency of the proposed optimization problem. The proposed ecological robustness-oriented approach with the above relaxations is then able to solve the bio-inspired power network design problem for *large synthetic* power system cases, with results evaluated for 200-, 500-, and 2000-bus synthetic grids, explicitly including the power system constraints. The optimized networks show that ecological robustness can be used to guide power grid network design with better network properties, reliability and maintaining the operational requirements.

The main contributions of this paper are as follows:

- A comprehensive study of ecological robustness applied to power grid network structure for large scale power system cases is presented. The results show that a design algorithm based on the ecological robustness trait strategically constructs the power grid network for reliability and survivability, with reduced violations under power grid measures of $N - x$ contingency analysis.
- The formulation of ecological robustness is relaxed using a Taylor Series Expansion, enabling a proposed scalable ecological robustness oriented power network expansion. This formulation is solved for four power system case studies with 24-, 200-, 500-, and 2000-bus systems respectively. These cases are *significantly* larger and more complex than those that have been previously been able to be studied.
- The original and optimized power grids are analyzed and compared regarding their network properties, such as robustness, node degree, centrality measures, etc., and reliability under different severities of contingencies. The increased robustness, increased node degree, reduced centrality measures, and reduced violations under contingencies highlight the networks' improvements resulting from the biological inspiration.

Section 2 presents related work applying ecological robustness in power network design. Section 3 presents a comprehensive study of ecological robustness applied to power network structure. Section 4 introduces the proposed mixed-integer nonlinear optimization problem and the relaxation scheme. Section 5 applies the relaxed bio-inspired network expansion to four power grids with 24-, 200-, 500-, and 2000-bus systems respectively. Section 6 analyzes the optimized networks regarding network properties, such as robustness, node degree, clustering coefficient, betweenness centrality measures,

etc., and system reliability under different levels of contingencies. Discussions are in Section 7 and Section 8 concludes the paper.

2. Related Work

The quantification of ecosystem robustness using information theory is presented in [22]. **Ecological Robustness**, R_{ECO} , is formulated as a function of two opposing but complementary attributes: *unutilized reserve capacity* that can be thought of as pathway redundancy and *effective performance* or pathway efficiency, with Equations (1-4).

$$R_{ECO} = -\left(\frac{ASC}{DC}\right) \ln\left(\frac{ASC}{DC}\right) \quad (1)$$

$$DC = -TSTp \sum_{i=1}^{N+3} \sum_{j=1}^{N+3} \left(\frac{T_{ij}}{TSTp} \log_2 \left(\frac{T_{ij}}{TSTp} \right) \right) \quad (2)$$

$$ASC = -TSTp \sum_{i=1}^{N+3} \sum_{j=1}^{N+3} \left(\frac{T_{ij}}{TSTp} \log_2 \left(\frac{T_{ij} TSTp}{T_i T_j} \right) \right) \quad (3)$$

$$TSTp = \sum_{i=1}^{N+3} \sum_{j=1}^{N+3} T_{ij} \quad (4)$$

where **Development Capacity** (DC) is the maximum amount of aggregated uncertainty that a network can have [26]; **Ascendency** (ASC) reflects the order or dependence between events [27]; and **Total System Throughput** ($TSTp$) is the system size, measured by total units circulated [28].

Calculating R_{ECO} requires information contained in the *Ecological Flow Matrix* (EFM) [\mathbf{T}], which is a square $(N+3) \times (N+3)$ matrix containing flow magnitude information between components in the network. N is the number of actors inside the system boundaries and the extra entries represent the system inputs, useful system exports, and dissipation or system exports that are lost [29]. The formulation of R_{ECO} quantifies robustness as a function of pathway *redundancy* and *efficiency*, which has been shown in ecosystems to be directly related to their long-term survival [22].

Ecosystems and power systems share a lot of commonalities regarding energy transition, sustainability of energy usage, and a required resilience against disruptions. Modeling power systems as analogous to a food web, which is a prey-predator model of an ecosystem,

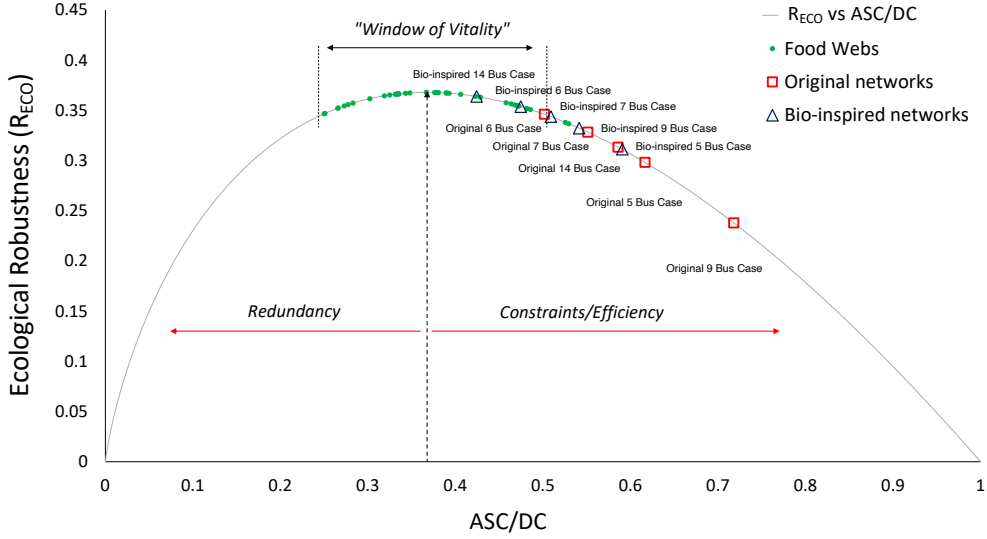


Figure 1: The ecological robustness curve depicting the five grids and their bio-inspired optimized versions, as well as a set of 38 food webs. Replicated from [21].

has been shown to enable the construction of an *Ecological Flow Matrix* with real power flow for ecological robustness optimization and analysis [20, 21]. The analogy between power grids and food webs sets the food web *actors* as corresponding to power grid components such as generators and buses. The *system inputs* correspond to energy supplied to generators from outside the system boundaries. The *useful exports* are the consumer loads (consumption) and the *dissipation* are power losses the system experiences. The entries in $[T]$ are notated as T_{ij} and represent the directed flow from node i to node j , corresponding to real power flows.

Figure 1 shows the R_{ECO} curve for five small power grid case studies alongside their biologically-optimized versions [21] and a set of 38 food webs. The ecological robustness of original power networks can be seen to be much lower than that of food webs, indicating the grid network structure has less pathway redundancy in comparison to these biological networks. The biologically-optimized power networks, which were redesigned to maximize R_{ECO} while still meeting all loads, successfully increased their ecological robustness in all cases by restructuring the grid with additional and altered pathways between components. The optimization done in [21] found that the resultant shift towards a higher R_{ECO} improved the reliability of all the grids under $N-1$, $N-2$, and $N-3$ contingencies. Figure 2 shows the normalized power system violations for original and bio-optimized power networks under contingencies. For

power systems, the power flow on branches, both transformers and transmission lines, and the voltage on buses should be maintained within their physical and operating limits [30]. For $N-x$ contingency analysis, if there is one branch's power flow is over the limit or the voltage magnitude is out of the required limit, it is counted as **one** violation. The violations can be seen to have been reduced by the bio-inspired redesigns in all of the 5 grid cases. While promising, this prior work [20, 21] unfortunately was unable to apply the bio-inspired optimization efficiently enough to make it applicable to large power system cases - resulting in an inability to study the potential success of the approach for more realistically sized grids.

A promising approach preliminarily investigated in [24] was to use `PowerModels.jl` [25] to combine the bio-inspired power network problem with its network expansion problem. The proposed MINLP in [24] integrates the power flow constraints with ecological robustness as the objective function. Unlike the optimization problem in [20, 21] that searches all possible network structures, the MINLP approach defines the possible connections to improve the efficiency while sacrificing a globally-optimal solution. Comparing the results in [24] and [21], the MINLP solution improves the network reliability under $N-1$ contingency and solves significantly faster. However, the optimization formulation in [24] fails to capture the feasible space, since Equations 1-3 involve the logarithm function (whose inputs

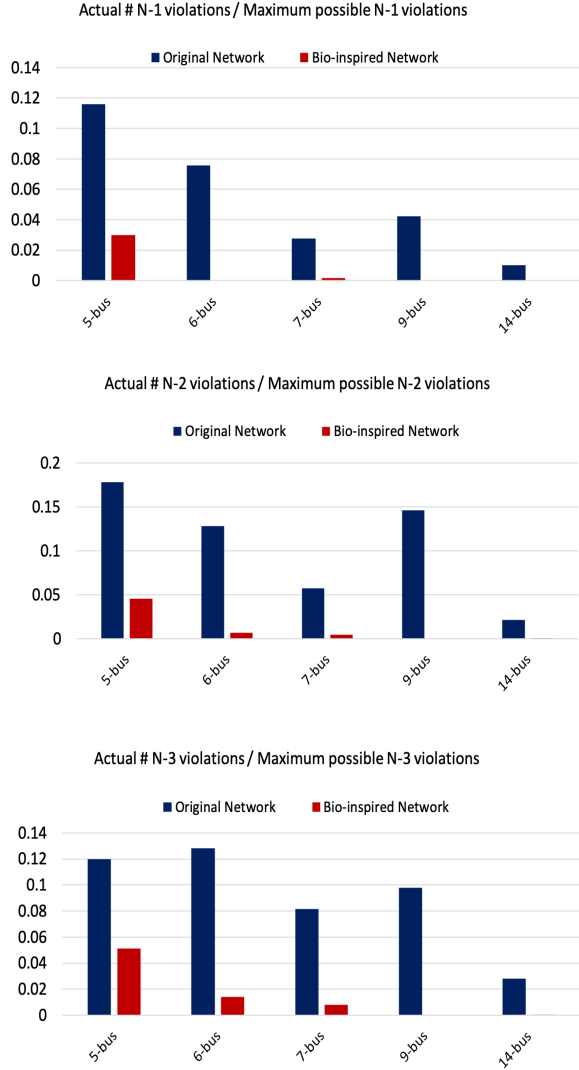


Figure 2: Reliability improvement for bio-inspired networks and original networks under N-1, N-2 and N-3 contingencies. Replicated from [21].

must be positive), while the input for R_{ECO} is power flow (whose direction can change during the solving process and making entries of T_{ij} become negative). This creates a problem for large cases where flow direction changes are more prevalent.

This paper relaxes the formulation of R_{ECO} based on the Taylor Series Expansion for the logarithm function making it able to solve a relaxed MINLP for the IEEE 24 Bus Reliability Test System (RTS)[31] and the synthetic 200-, 500-, and 2000-bus power grids from [32].

3. Ecological Robustness and Power Network Structure

Ecological robustness was first applied to power grids with the goal of creating a “bio-inspired” network design in [21], showing that the resultant biologically-optimized networks improved both the robustness and reliability of the grids. Understanding if the biological optimization inherently adds value to the design of power grids is difficult, however, as for the small-scale cases tested in that work all resulted in branches being added, and added branches will almost certainly improve grid reliability somewhat. This leaves the question: with a *set* number of lines available, can ecological robustness create a more resilient grid? The relationship among added links, network structure, and ecological robustness in power systems needs to be better understood. A comprehensive study of ecological robustness is thus performed in this section, highlighting the resultant power system structures with different number of links for all the cases from [21]. The results confirm from an engineering perspective that ecological robustness is a function of the number of links, the network’s structure, and its function (power flows).

Figure 3 shows the results for a 5-, 6-, 7-, 9-, and 14-bus case when links are added to the original structure until all buses are connected and all possible network structures have been considered. The corresponding ecological robustness is then calculated for each topology. For example, the original 5-bus case has 7 links (5 branches connecting buses and 2 links connecting a bus and generator). Since the connection between bus and generator is already one-to-one, added links only occur between buses. One link is added to the original network in every possible location and the power flow for the new network structure is calculated (for which electrical parameters, such as resistance, reactance, limits, etc., must be assigned to the new branches). For simplification, the mean value of the existing branches’ electrical parameters are used. The ecological robustness is then calculated for each architecture.

The 5-bus, 6-bus, and 7-bus cases cover every possible new architecture for each added link. The 9-bus and 14-bus cases however can have thousands of different structures for each number of links. Thus, a uniform distribution of network structures under a certain number of links is assumed. Each network architecture has a unique ecological robustness thus the ecological robustness for a set number of links also has a uniform distribution [33]. 150 network structures were randomly selected from all possible network structures for the 9- and 14-bus cases to represent the relationship between

ecological robustness and added links.

Figure 3 supports that while increasing the number of links in the network does generally enable a higher *maximum* ecological robustness, the maximum R_{ECO} does not correspond to the grid architecture with the most links (Figure 3b-e). These results confirm that using ecological robustness as a design guideline can *guide* the placement of new links and maximizing R_{ECO} does more than just *add* links: different network structures have different ecological robustness with a variance around 5%. Moreover, adding unnecessary links can reduce ecological robustness - or just because more links are added does not ensure that R_{ECO} will increase. These results show that ecological robustness metric, and the characteristic of biological food webs to maximize R_{ECO} with a unique balance of pathway efficiency vs. redundancy, can be a non-obvious design guideline for selecting power flow pathways such that it strategically guides the network construction for reliability and survivability.

4. Ecological Robustness Oriented Power Network Expansion

A mixed-integer nonlinear optimization model for ecological robustness oriented power network expansion was proposed in [24], where the optimization model constructs the power networks to achieve the maximal ecological robustness while maintaining power flow constraints. This section reviews the mixed-integer nonlinear programming problem (MINLP) model and presents the relaxation scheme using a Taylor Series Expansion for the logarithm function to solve the problem for large power systems.

4.1. Mixed-Integer Optimization Model

The ecological robustness oriented power network expansion problem is built upon the Transmission Network Expansion Planning (TNEP) problem and implemented using PowerModels.jl with the objective of achieving optimal ecological robustness (R_{ECO}). The ecological robustness is calculated through [T], whose entries are generator power outputs, branch power flows, losses, and load. The TNEP problem is formulated as a mixed-integer optimization problem where each candidate branch has a binary decision variable α_{ij} for the candidate branch from bus i to bus j . The initial value of α_{ij} = zero means the corresponding branch does not exist in the original network. If the resulting α_{ij} after optimization equals one, the branch is built to reach a maximum R_{ECO} .

Algorithm 1 Ecological Robustness Oriented Power Network Expansion

Variables:

V_i ($\forall i \in M$), θ_i ($\forall i \in M$), P_{gen_i} ($\forall i \in G$), Q_{gen_i} ($\forall i \in G$), $\alpha_{ij} \in \{0,1\}$ ($\forall (i,j) \in NB$)

Objective:

$$Max(R_{ECO} = f(\mathbf{EFM})) \quad (5a)$$

Subject to:

$$\mathbf{EFM} = \mathbf{T}(P_{ij}, P_{gen_i}, P_{load_i}, P_{loss_i}, \alpha_{ij}) \quad (5b)$$

$$v_i^l \leq V_i \leq v_i^u \quad (\forall i \in M) \quad (5c)$$

$$s_{ij}^l \leq S_{ij} \leq s_{ij}^u \quad (\forall (i,j) \in B \cup NB) \quad (5d)$$

$$s_{gen_i}^l \leq S_{gen_i} \leq s_{gen_i}^u \quad (\forall i \in G) \quad (5e)$$

$$S = P + iQ \quad (5f)$$

$$P_{ij} = V_i^2[-G_{ij}] + V_i V_j [G_{ij} \cos(\theta_{ij}) + B_{ij} \sin(\theta_{ij})] \quad (\forall (i,j) \in B) \quad (5g)$$

$$P_{ij} = \alpha_{ij} V_i^2[-G_{ij}] + \alpha_{ij} V_i V_j [G_{ij} \cos(\theta_{ij}) + B_{ij} \sin(\theta_{ij})] \quad (\forall (i,j) \in NB) \quad (5h)$$

$$Q_{ij} = V_i^2[B_{ij}] + V_i V_j [G_{ij} \sin(\theta_{ij}) - B_{ij} \cos(\theta_{ij})] \quad (\forall (i,j) \in B) \quad (5i)$$

$$Q_{ij} = \alpha_{ij} V_i^2[B_{ij}] + \alpha_{ij} V_i V_j [G_{ij} \sin(\theta_{ij}) - B_{ij} \cos(\theta_{ij})] \quad (\forall (i,j) \in NB) \quad (5j)$$

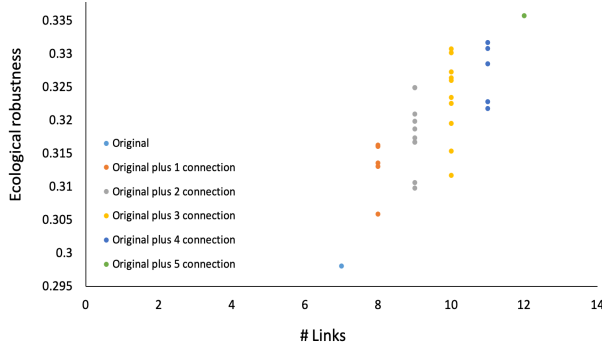
$$P_i = P_{load_i} - P_{gen_i} = \sum_j P_{ij} \quad (\forall j \in M) \quad (5k)$$

$$Q_i = Q_{load_i} - Q_{gen_i} = \sum_j Q_{ij} \quad (\forall j \in M) \quad (5l)$$

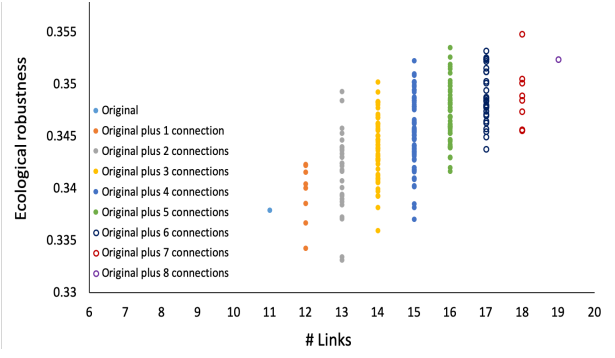
$$P_{loss_i} = \frac{1}{2} \sum_j (P_{ij}^2 + Q_{ij}^2) / (B_{ij} V_i^2) \quad (\forall j \in M) \quad (5m)$$

where **EFM** is *Ecological Flow Matrix*, B is the set of existing branches, NB is the set of candidates of new branches, M is the set of buses, and G is the set of generators. The i in Equation (5f) is a imaginary number.

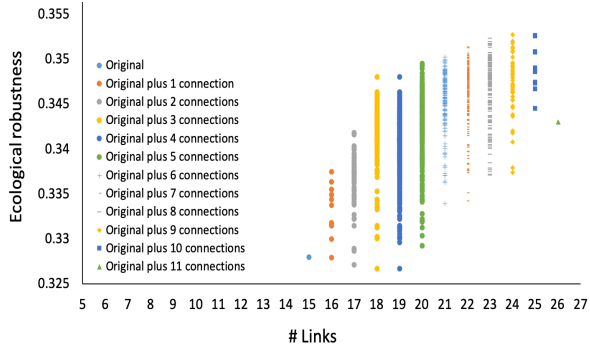
The proposed *Ecological Robustness Oriented Power Network Expansion Problem* is formulated in Algorithm 1 under the AC power flow model. The objective func-



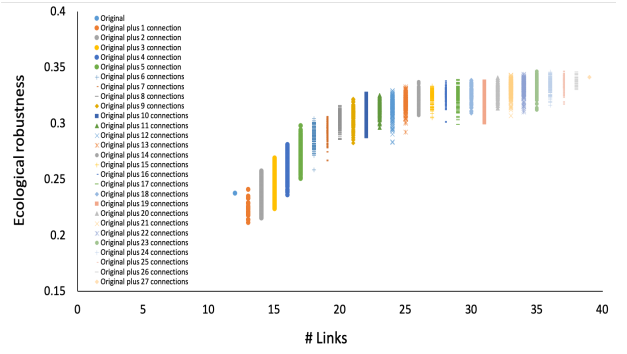
(a) 5-bus case



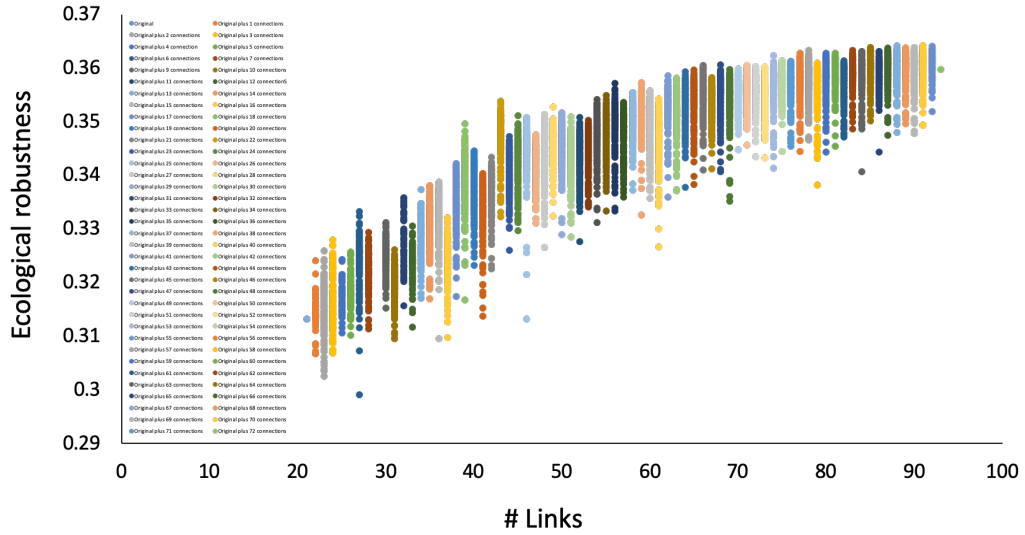
(b) 6-bus case



(c) 7-bus case



(d) 9-bus case



(e) 14-bus case

Figure 3: The ecological robustness with the increase number of links for the 5-bus, 6-bus, 7-bus, 9-bus and 14-bus power system cases in [21].

tion (5a) is formulated through Equation (1)-(4). The input of the objective function is $[T]$, which consists of generator real power output P_{gen_i} , real power flow P_{ij} from existing branches and candidate branches, power consumption at each load P_{load_i} , power loss P_{loss_i} at each bus, and binary decision variables α_{ij} for candidate branches. Figure 4 illustrates the formulation of $[T]$ with the above entries. Matrix $[T]$ gives the energy transitions among actors and extra system inputs, useful exports and dissipation. The system inputs are from generators, so the first row consists of P_{gen_i} . Generators and buses are modeled as actors, so the energy transitions between them are also P_{gen_i} . Among buses, the energy transitions are filled with P_{ij} and P_{neij} , where the P_{ij} are the existing branches' power flows and P_{neij} are the candidate branches' power flows depending on the decision variable α_{ij} ($P_{neij} = \alpha_{ij} P_{ij}$ for candidate branches). The outputs are the loads at each bus, which are the fixed value of P_{load_i} . The dissipation are the energy loss at each actor.

The dissipation at each generator is modeled as zero since the generators send power directly to the system. However, it is worthwhile to mention that the energy dissipation caused by generating electricity from various sources *can* be considered in this model for further assessment. Buses do not have energy dissipation but the branches connected to the bus do, thus the branch losses for each bus are aggregated using Equation (5m) to formulate the P_{loss_i} , which also depends on the power flow dispatch. A more indepth investigation of the modeling process for line losses when lines are modeled as directional graph nodes can be found in [34]. Equations (5c) - (5l) ensure the network structure is satisfied with power balance and power system operational constraints with the AC power flow model for real power (P) and reactive power (Q).

Power flow dispatch depends on the real (P_i) and reactive power (Q_i) injection at each bus, bus voltage (voltage magnitude V_i , voltage angle θ_i), and the network structure [35]. Variables for the proposed problem include each generator's real and reactive power input P_{gen_i} and Q_{gen_i} , each bus' voltage magnitude V_i and voltage angle θ_i , and the binary decision variable α_{ij} for candidate branches. The Ecological Robustness Oriented Power Network Expansion Problem can thus optimize the network structure and power flow dispatch to maximize R_{ECO} .

4.2. Relaxation of the Ecological Robustness Formulation

This optimization problem becomes a MINLP problem with the binary decision variable α_{ij} and the for-

mulation of ecological robustness R_{ECO} : a typical class of NP-hard problems [36]. Moreover, for the logarithm function, the domain of the function must be positive. The input for Equations (1) - (3) depends on the power flow (P_{ij}) magnitude and direction. However, P_{ij} is solved based on V_i , θ_i , P_{gen_i} , Q_{gen_i} and α_i . During the optimization process, the solution is not guaranteed to fall in the domain for the logarithm function, which can make the model invalid. As in [24], when the proposed MINLP was solved for large cases or used the AC power flow model, it is unable to solve using the *Ipopt* [37], *Juniper* [38], and *Cbc* [39] tools because of an invalid mathematical model. Taylor Series Expansion of the natural logarithm function is thus used here to relax the formulation of ecological robustness for proposed problem's feasibility in larger power system cases.

There are several Taylor Series Expansions for the natural logarithm function. Considering the domain for the expansion, this paper utilizes the following relaxation, with $x > 0$ [40]:

$$\begin{aligned} \ln(x) &= 2 \sum_{n=1}^{\infty} \frac{((x-1)/(x+1))^{(2n-1)}}{(2n-1)} \\ &= 2 \left[\frac{(x-1)}{(x+1)} + \frac{1}{3} \left(\frac{(x-1)}{(x+1)} \right)^3 + \frac{1}{5} \left(\frac{(x-1)}{(x+1)} \right)^5 + \dots \right] \end{aligned} \quad (6)$$

The logarithm function has a base of 2 in Equations (2) and (3). Using a property of logarithm functions,

$$\log_2(x) = \frac{\ln(x)}{\ln(2)} \quad (7)$$

the Taylor Series Expansion of $\log_2(x)$ can be expanded:

$$\log_2(x) = \frac{2}{\ln(2)} \left[\frac{(x-1)}{(x+1)} + \frac{1}{3} \left(\frac{(x-1)}{(x+1)} \right)^3 + \frac{1}{5} \left(\frac{(x-1)}{(x+1)} \right)^5 + \dots \right] \quad (8)$$

Assuming the flow direction depends on the initial state, the flow direction of all power flows is defined and formulates the objective function under the domain requirement of $x > 0$ for a Taylor Series Expansion. Then, by adapting the first order Taylor Series Expansion of Equations (6) and (8) into Equation (1) - (3), the formulation of R_{ECO} is relaxed in Algorithm 1. The relaxed Ecological Robustness Oriented Power Network Expansion problem can then be applied to large power grid networks successfully (even with flow direction changes during the optimization process).

5. Case Studies

This section applies the relaxed Ecological Robustness Oriented Power Network Expansion for four power

		Gen 1	. . .	Gen n	Bus 1	. . .	Bus n	Output	Dissipation
Input	0	$P_{gen\ 1}$. . .	$P_{gen\ n}$	0	. . .	0	0	0
Gen 1	0	0	. . .	0	$P_{gen\ 1}$. . .	0	0	0
.
.
.
Gen n	0	0	. . .	0	0	0	$P_{gen\ n}$	0	0
Bus 1	0	0	. . .	0	0	. . .	P_{1n}	$P_{load\ 1}$	$P_{loss\ 1}$
.	$P_{ne\ 1i}$
.	P_{ij}	$P_{ne\ in}$.	.
.	$P_{ne\ ij}$.	.	.
Bus n	0	0	. . .	0	P_{n1}	. . .	0	$P_{load\ n}$	$P_{loss\ n}$
	0	0	. . .	0	0	. . .	0	0	0
	0	0	. . .	0	0	. . .	0	0	0

Figure 4: An example *Ecological Flow Matrix* [T] for a grid with n generators and m buses and grid customers residing outside the system boundaries (modeled as useful outputs). The P_{gen_i} is the real power output from generator i . Generators are treated as lossless so the dissipation column entries for the generators are zero. The real power consumption at Bus i is P_{load_i} . P_{loss_i} is the real power loss at Bus i . P_{ij} and $P_{ne_{ij}}$ are the real power flows at the corresponding branch and candidate branch. No connections and/or no power flow between grid components results in a matrix entry of zero.

system cases: the IEEE 24 Bus RTS [31] and three synthetic grids from [32] (ACTIVSg200 200-bus system, ACTIVSg500 500-bus system, and ACTIVSg2000 2000-bus system). The IEEE 24 Bus RTS is used for testing various reliability analysis methods. The synthetic cases are satisfied with the statistical characters of actual grids without compromising the confidentiality of real systems. They have been evaluated for topology connectivity, overlap with the Delaunay triangulation and minimum spanning tree of the substations, AC power flow convergence, and geographic intersections between same-voltage-level transmission lines [32]. However, these cases do not have the data for network expansion. This section introduces an algorithm to generate candidate branches for synthetic grids and solves the Ecological Robustness Oriented Power Network Expansion problem for each.

5.1. Use Case Creation

The proposed Ecological Robustness Oriented Power Network Expansion is built upon the TNEP problem in `PowerModels.jl`, which requires the information of candidate branches. The original synthetic grids do not have the candidate branches to expand the network, so we use the Algorithm 2 to create the candidate branches based on the existing grid information. In power system modeling, the construction of transformers will create extra buses, so the candidate branches in this paper created by Algorithm 2 are transmission lines that connect buses at the same voltage level.

Algorithm 2 provides a *Naive* way to create the candidate branches by connecting buses at the same voltage

level. The algorithm assumes the candidate branches follow a uniform distribution. The input for Algorithm 2 is the case's bus and branch information. Algorithm 2 classifies the existing branches into different voltage levels and generates normal distributions for different parameters at each voltage level. The normal distribution is always used to represent the real-valued random variables. With the *mean* and *variance* of existing branches' parameters, the generated normal distribution can be used to select the candidate branches' parameters to fit with the original case. The synthetic grids have hundreds of buses, resulting in a huge number of possible branches. Thus, all possible branches are assumed to have the same probability to be selected and the algorithm selects M candidate branches from all possible branches. As in Section 3, even with random sampling, R_{ECO} is able to select a network construction with an ecologically-similar balance of pathway efficiency and redundancy. Algorithm 1 can guide the network expansion with candidate branches from Algorithm 2 to achieve the optimal ecological robustness. Additional information such as geographic location, cost, and government policies can further improve the realism when considering different candidate branches.

5.2. Results

Algorithm 1 is applied to four power system cases (the IEEE 24 Bus Reliability RTS and three synthetic grids) to redesign their network under the guidance of ecological robustness R_{ECO} . Since these grids do not have candidate branch information, Algorithm 2 created 50, 100, 150, and 200 candidate branches for each

Algorithm 2 Create Candidate Branches for Network Expansion Problem

Input = All branches' information from the case, the total number of candidate branches (M)
 Classify branches based on the voltage level
while The number of candidate branches $< M$ **do**
 for Each Voltage Level **do**
 Collect the branch information for all parameters
 Compute the *mean* (μ) and *variance* (σ^2) for each parameter
 Generate a *Normal Distribution* ($N(\mu, \sigma^2)$) for each parameter
 Randomly select the *from bus* and *to bus* at the same voltage level to create a candidate branch
 Insert the parameter for the candidate branch using the *Parameters' Normal Distribution* ($N(\mu, \sigma^2)$).
 end for
end while
 Branch information includes electrical parameters (such as voltage level, resistance, reactance, capacitance, etc.) and operating parameters (such as thermal limits, ratings, etc).

case, respectively (each grid has a unique set of candidate branches). All scenarios are solved with both AC and DC power flow models.

The DC power flow model treats the system as lossless with $\mathbf{G} = \mathbf{0}$ and voltage magnitudes of all buses are assumed constant at 1.0 per unit. Additionally, the angle difference between two buses is small, such that $\cos(\theta_{ij}) = 1$ and $\sin(\theta_{ij}) = \theta_i - \theta_j$ [35]. Thus, $\mathbf{Q} = \mathbf{0}$ and the Equation (5i), (5j), and (5l) can be removed from Algorithm 1. Equation (5g) and (5h) can be simplified as:

$$P_{ij} = B_{ij}(\theta_i - \theta_j) \quad (\forall (i, j) \in B) \quad (9)$$

$$P_{ij} = \alpha_{ij}B_{ij}(\theta_i - \theta_j) \quad (\forall (i, j) \in NB) \quad (10)$$

For transmission networks, there are different voltage ratings in the system. The higher the voltage rating is, the further the power can be transferred. The highest voltage transmission lines are the backbone of transmission network. Thus, the candidate branches are selected with the highest voltage ratings. As mentioned earlier, the proposed algorithm not only solves the network structure, it also solves the optimal power flow dispatch with a output vector of generator setpoints. The resultant network design is analyzed with both the optimized network structure and the optimized network

structure with optimal power flow. The naming convention used for each network follows the pattern of *Original Case Name-Number of Candidate Branches-Structure/OPF*. The *-Structure* means the network only optimizes its network structure from Algorithm 1. The *-OPF* means the network optimizes its network structure and power flow dispatch from Algorithm 1.

The solver for the MINLP problem uses the *Ipopt* [37], *Juniper* [38], and *Cbc* [39]. *Ipopt* is a library for large scale nonlinear optimization for continuous systems. *Juniper* provides a heuristic solution for non-convex problems. *Cbc* is an open-source mixed integer programming solver. All the problems were solved using a laptop with a 2.4 GHz processor and 8 GB memory.

5.2.1. IEEE 24 Bus Reliability Test System (RTS)

The IEEE 24 Bus Reliability Test System (RTS) [31] has 24 buses and 37 branches. The online generation limits are 3405 MW and 1776 MVAR for real and reactive power respectively, and they support 2850 MW and 580 MVAR load in the system. With 24 buses, there are 276 links that can be selected as candidate branches to expand the network structure. After applying both the DC and AC power flow models for four scenarios with 50, 100, 150 and 200 candidate branches respectively, the problem can only be solved using the DC power flow model with the termination status of **Locally Solved**. With the AC power flow model, the termination status is **LOCALLY INFEASIBLE** without the solution of the proposed problem. Thus, the results in Table 1 are solved by the DC power flow model only. Fig. 5 shows the network structure with expansion from the original 24 bus case to the ecological robustness oriented network considering 50 candidate branches. Fig. 5(a) is the original topology of 24 Bus RTS; the blue links in Fig. 5(b) are the candidate branches for 24 Bus RTS; the red links in Fig. 5(c) are branches built under the guidance of optimal ecological robustness.

Table 1 lists all the scenarios for the IEEE 24 Bus RTS with different numbers of candidate branches that when solved resulted in the same R_{ECO} value of 0.3431 for the **Optimal R_{ECO}** from the *Ipopt* solver. The **Optimal R_{ECO}** is the mathematical optimal value solved from the model of Algorithm 1 with the relaxation of Equation (8). The relaxed formulation of R_{ECO} with Equation (8) means that the real R_{ECO} achieved in each case can be different. Thus, R_{ECO} is recalculated for each case based on its optimized network structure and power flows, as listed in column **Achieved R_{ECO}** . The results of **Achieved R_{ECO}** show that the optimized networks have a higher R_{ECO} than the original case and the

Table 1: Results of Ecological Robustness Oriented Power Network Design for IEEE 24 Bus Reliability Test System

Use Case	Solved Status	Solved Optimal R_{ECO}	Achieved R_{ECO}	Number of Candidate Branches	Number of Built Branches	Computation Time(seconds)
IEEE 24 Bus RTS	NA	NA	0.3362	0	0	0
IEEE 24 Bus RTS-50-Structure	LOCALLY SOLVED	0.3431	0.3485	50	21	1.74
IEEE 24 Bus RTS-50-OPF	LOCALLY SOLVED	0.3431	0.3491	50	21	1.74
IEEE 24 Bus RTS-100-Structure	LOCALLY SOLVED	0.3431	0.3509	100	25	8.54
IEEE 24 Bus RTS-100-OPF	LOCALLY SOLVED	0.3431	0.3498	100	25	8.54
IEEE 24 Bus RTS-150-Structure	LOCALLY SOLVED	0.3431	0.3446	150	12	75.90
IEEE 24 Bus RTS-150-OPF	LOCALLY SOLVED	0.3431	0.3455	150	12	75.90
IEEE 24 Bus RTS-200-Structure	LOCALLY SOLVED	0.3431	0.3464	200	8	23.017
IEEE 24 Bus RTS-200-OPF	LOCALLY SOLVED	0.3431	0.3473	200	8	23.017

-OPF networks have a higher R_{ECO} than the -Structure networks (except for the 100 candidate branch scenario). The number of built branches does not increase with increasing numbers of candidate branches. This confirms that the proposed Algorithm 1 utilizes the R_{ECO} to *strategically* construct the network structure to improve the system's R_{ECO} and maintain power system constraints.

5.2.2. ACTIVSg200

The ACTIVSg200 [32] has 200 buses and 246 branches with 3426.84 MW and 1346.57 MVAR online generation limits to support 2178.05 MW and 620.68 MVAR load in the system. With 200 buses, there are 19900 links that can be selected as candidate branches to expand the network structure. After applying both DC and AC power flow models for four scenarios with 50, 100, 150 and 200 candidate branches respectively, the problem can only be solved using the DC power flow model with the termination status of **Locally Solved**. With the AC power flow model and increasing the *max.iter* to 50000, the solver stops due to **Restoration Failed** without any solution. Thus, the results in

Table 2 are solved by the DC power flow model only. Fig. 6 shows the network structure expands from the original 200 bus case to the ecological robustness oriented network with 50 candidate branches. Fig. 6(a) is the original topology of ACTIVSg200; the blue links in Fig. 6(b) are the candidate branches for ACTIVSg200; the red links in Fig. 6(c) are branches built under the guidance of optimal ecological robustness.

In Table 2, the results for the ACTIVSg200 cases are similar to the IEEE 24 Bus RTS. The solved **Optimal R_{ECO}** is 0.3431 for all scenarios, but the **Achieved R_{ECO}** values are smaller. Considering there are 19900 possible links, the created 200 candidate branch may not have the optimal structure. However, the optimized networks show improved network properties and reliability, which is further discussed in the next section. For the ACTIVSg200 cases, all -OPF networks have higher than their corresponding -Structure networks. Also, the number of built branches do not increase with the increasing of candidate branches.

Table 2: Results of Ecological Robustness Oriented Power Network Design for ACTIVSg200

Use Case	Solved Status	Solved Optimal R_{ECO}	Achieved R_{ECO}	Number of Candidate Branches	Number of Built Branches	Computation Time(seconds)
ACTIVSg200	NA	NA	0.2450	0	0	0
ACTIVSg200-50-Structure	LOCALLY SOLVED	0.3431	0.2643	50	26	58.64
ACTIVSg200-50-OPF	LOCALLY SOLVED	0.3431	0.2650	50	26	58.64
ACTIVSg200-100-Structure	LOCALLY SOLVED	0.3431	0.2590	100	15	35.46
ACTIVSg200-100-OPF	LOCALLY SOLVED	0.3431	0.2591	100	15	35.46
ACTIVSg200-150-Structure	LOCALLY SOLVED	0.3431	0.2548	150	5	84.09
ACTIVSg200-150-OPF	LOCALLY SOLVED	0.3431	0.2548	150	5	84.09
ACTIVSg200-200-Structure	LOCALLY SOLVED	0.3431	0.2701	200	51	45.80
ACTIVSg200-200-OPF	LOCALLY SOLVED	0.3431	0.2702	200	51	45.80

5.2.3. ACTIVSg500

The ACTIVSg500 [32] has 500 buses and 599 branches with 6455.78 MW and 3899.35 MVAR online generation limits to support 5001.67 MW and 1333.8 MVAR load in the system. With 500 buses, there are 124750 links can be selected as candidate branches to expand the network structure. After applying the both DC and AC power flow models for four scenarios (50, 100, 150 and 200 candidate branches, respectively), the problem can only be solved using a DC power flow model with the termination status of **Locally Solved**. The AC power flow model and increasing the *max_iter* to 50000, the solver stops due to **Restoration Failed** without any solution. Thus, the results in Table 3 are from the DC power flow model. Figure 7 shows the network structure expands from the original ACTIVSg500 case to the ecological robustness oriented network with 50 candidate branches. Figure 7(a) is the original topology of ACTIVSg500; the blue links in Figure 7(b) are the candidate branches for ACTIVSg500; the red links in Figure 7(c) are branches built under the guidance of optimal ecological robustness.

The results for the ACTIVSg500 cases are in Table 3, which is similar to the ACTIVSg200 case. The solved **Optimal R_{ECO}** is 0.3431 for all scenarios, but the **Achieved R_{ECO}** are smaller. Considering there are 124750 possible links, the created 200 candidate branch may not have the optimal structure. Moreover, with 200 candidate branches, the optimized network doesn't build new branch. The computation time for the *ACTIVSg500-200-OPF* is much longer than other scenarios. Compared with other cases, far fewer branches are added in the ACTIVSg500 case.

5.2.4. ACTIVSg2000

The ACTIVSg2000 [32] has 2000 buses and 3206 branches with 6455.78 MW and 3899.35 MVAR online generation capability to support 5001.67 MW and 1333.8 MVAR load in the system. 2000 buses results in 1999000 links that can be selected as candidate branches to expand the network's structure. After applying the both DC and AC power flow models for four scenarios (50, 100, 150 and 200 candidate branches, respectively), the problem was again found to only be solvable using a DC power flow model with the termi-

Table 3: Results of Ecological Robustness Oriented Power Network Design for ACTIVSg500

Use Case	Solved Status	Solved Optimal R_{ECO}	Achieved R_{ECO}	Number of Candidate Branches	Number of Built Branches	Computation Time(seconds)
ACTIVSg500	NA	NA	0.2132	0	0	0
ACTIVSg500-50-Structure	LOCALLY SOLVED	0.3431	0.2198	50	2	127.40
ACTIVSg500-50-OPF	LOCALLY SOLVED	0.3431	0.2198	50	2	127.40
ACTIVSg500-100-Structure	LOCALLY SOLVED	0.3431	0.2149	100	1	84.61
ACTIVSg500-100-OPF	LOCALLY SOLVED	0.3431	0.2214	100	1	84.61
ACTIVSg500-150-Structure	LOCALLY SOLVED	0.3431	0.2228	150	14	84.61
ACTIVSg500-150-OPF	LOCALLY SOLVED	0.3431	0.2227	150	14	84.61
ACTIVSg500-200-OPF	LOCALLY SOLVED	0.3431	0.2220	200	0	1091.35

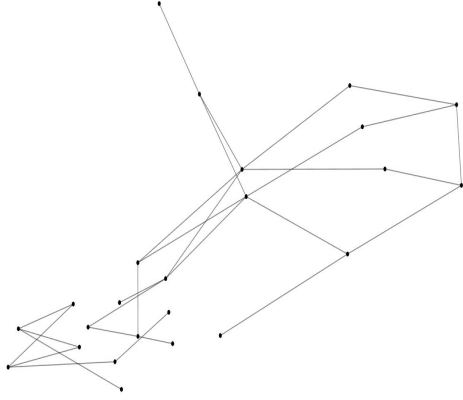
Table 4: Results of Ecological Robustness Oriented Power Network Design for ACTIVSg2000

Use Case	Solved Status	Solved Optimal R_{ECO}	Achieved R_{ECO}	Number of Candidate Branches	Number of Built Branches	Computation Time(hours)
ACTIVSg2000	NA	NA	0.2346	0	0	0
ACTIVSg2000-50-OPF	LOCALLY SOLVED	0.3431	0.2346	50	0	5.73
ACTIVSg2000-100-OPF	LOCALLY SOLVED	0.3431	0.2346	100	0	6.49
ACTIVSg2000-150-OPF	LOCALLY SOLVED	0.3431	0.2345	150	0	10.12
ACTIVSg2000-200-OPF	LOCALLY SOLVED	0.3431	0.2343	200	0	15.18

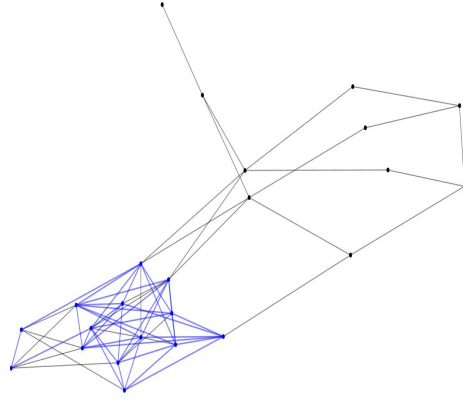
nation status of **Locally Solved**. The AC power flow model and increasing the *max_iter* to 50000 gives an output of **Restoration Failed** without any solution.

The results for the ACTIVSg2000 cases are in Table 4 solved with DC power flow model. The solved **Optimal R_{ECO}** is 0.3431 for all scenarios, but no new branches

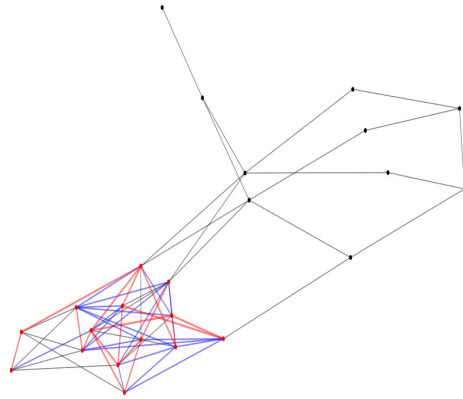
are added in any of the scenarios and the computation time is much longer than in the other cases. Moreover, the optimized networks their **Achieved R_{ECO}** are lower than the original network. However, this doesn't mean the structure of ACTIVSg2000 case is **ecologically optimal**. The R_{ECO} of the ACTIVSg2000 cases are still



(a) Original IEEE 24 Bus RTS network topology



(b) Original IEEE 24 Bus RTS network topology with 50 candidate branches (in blue)



(c) Ecological robustness-oriented IEEE 24 Bus RTS network topology with new constructed branches (in red)

Figure 5: IEEE 24 Bus RTS ecological robustness-oriented network expansion with 50 candidate branches

ality". Since we only consider 200 candidate branches using Algorithm 2, which is only a small portion from all candidate branches, the optimal network structure is identified from them.

The computation time for the ACTIVSg500-200-OPF and cases in ACTIVSg2000 were significantly longer as compared to the other grid test cases. It suggests that the proposed MINLP problem can be solved very efficiently with a DC power flow model when the model is solved to optimize the network structure rather than optimize the power flow dispatch. This depends on the set of candidate branches. If the optimal network structure can be identified from the candidate branches, the model is solved as optimizing the network structure. If the optimal network structure is not identified with the candidate branches, the model will search all possible network structure and optimize the power flow, which cause the computation time much longer.

6. Network Analyses

The optimized networks are analyzed and compared with their original network based on their network properties and power system reliability using PowerWorld Simulator [41] and Easy SimAuto [42]. A simplified, cost-effective analysis is also presented for both the optimized network and original network. Since the structure of ACTIVSg2000 is not optimized, the analyses are focused on the IEEE 24 Bus RTS, ACTIVSg200, and ACTIVSg500.

Even though the proposed MINLP problem is only solved with DC power flow model, the optimized network and the optimized network with OPF are analyzed in the AC power flow model in PowerWorld Simulator [41]. All cases are initially solved using AC power flow model without any violations to examine the cases' ability of absorbing disturbances.

6.1. Network Properties Comparison

Another entropy based network robustness metric (R_{CF}) is used to identify cascading failures in power systems in [43]. The calculation of R_{CF} is based on the power flow and network topology in the system as in Equation (11)-(15):

$$p_i = \frac{f_i}{\sum_{j=1}^L f_j} \quad (11)$$

$$\alpha_i = \frac{1}{LL_i} \quad (12)$$

outside of the ecological networks' "window of vi-

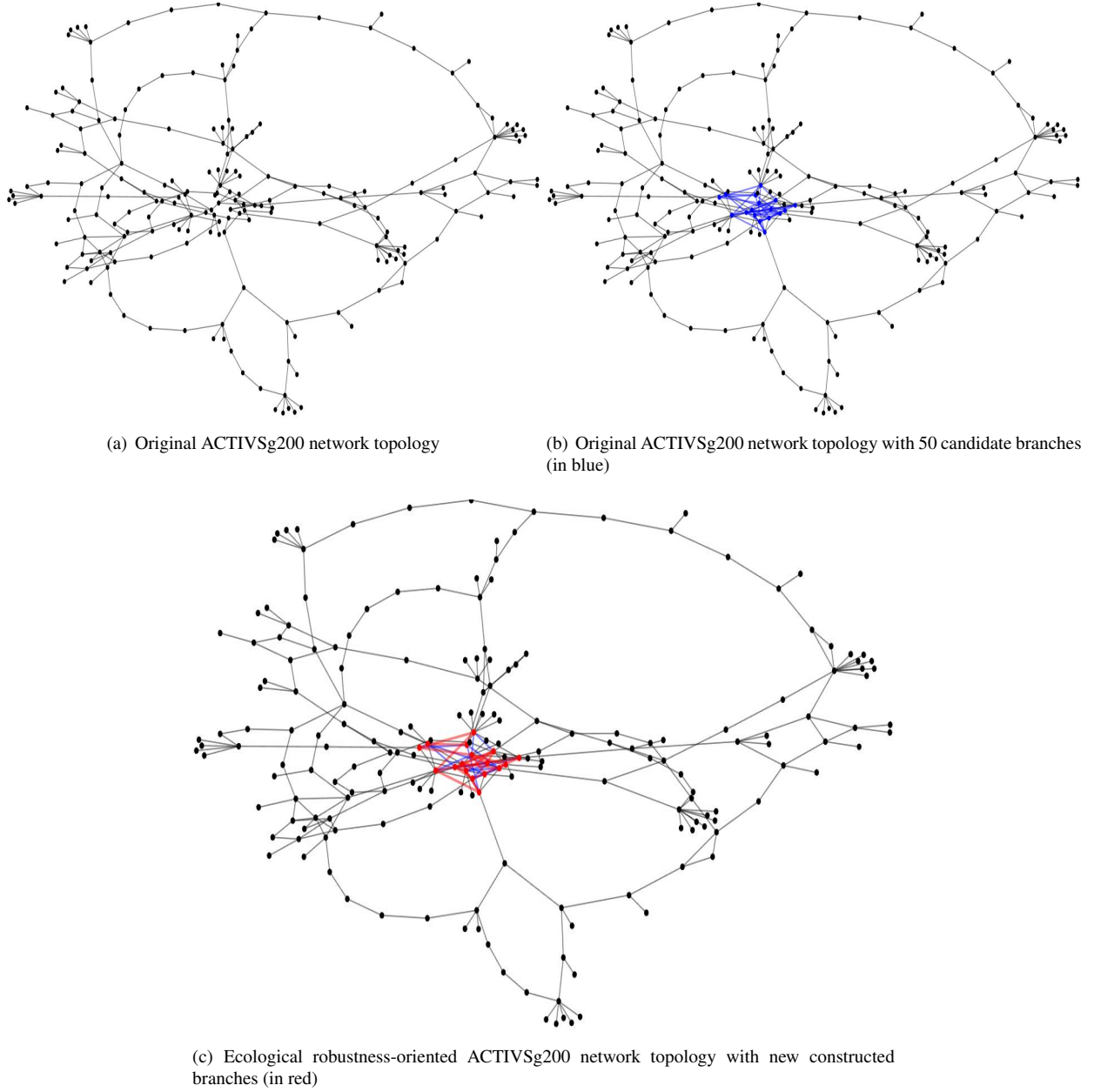


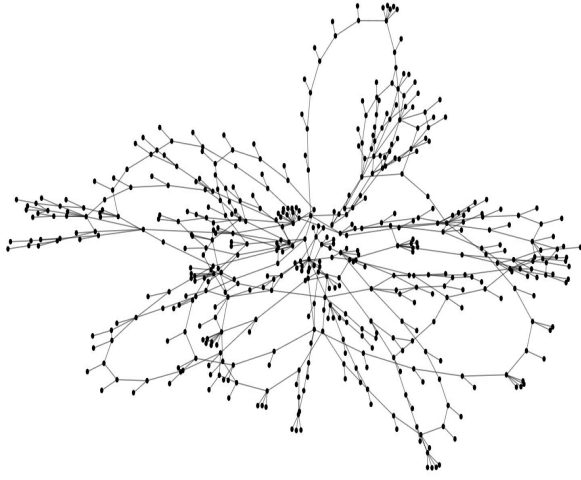
Figure 6: ACTIVSg200 ecological robustness-oriented network expansion with 50 candidate branches

$$R_{n,j} = - \sum_{i=1}^L \alpha_i p_i \log(p_i) \quad (13)$$

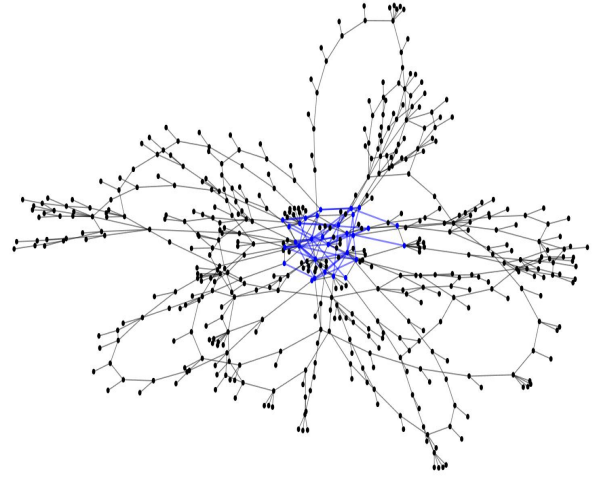
$$\delta_i = \frac{P_i}{\sum_{j=1}^N P_j} \quad (14)$$

$$R_{CF} = \sum_{i=1}^N R_{n,i} \delta_i \quad (15)$$

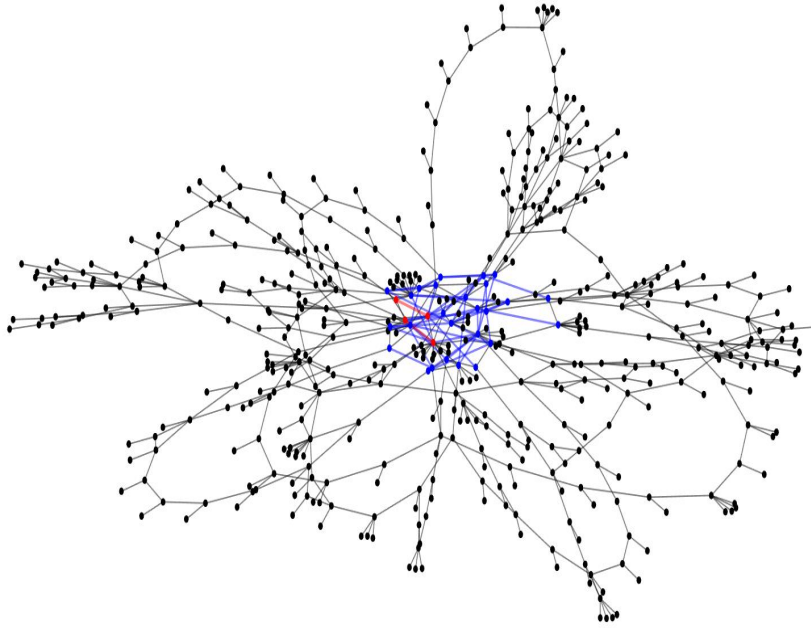
where f_i in Equation (11) is the power flow at line i and p_i is the normalized flow values on the out-going links; LL_i in Equation (12) is the loading level, which is the ration between the load and the maximum capacity of the corresponding line i ; P_i in Equation (14) is the total power distributed by node i and N is the number of nodes in the network. With higher value of R_{CF} , the network is more robust and less likely has cascading failure



(a) Original ACTIVSg500 network topology



(b) Original ACTIVSg500 network topology with 50 candidate branches (in blue)



(c) Ecological robustness-oriented ACTIVSg500 network topology with new constructed branches (in red)

Figure 7: ACTIVSg500 ecological robustness-oriented network expansion with 50 candidate branches

[43].

All networks are analyzed here with typical complex network properties, including the average node degree (\bar{d}), clustering coefficient (\bar{c}), average betweenness centrality measures (\bar{b}) and average shortest path (\bar{l}). The power flow distribution is investigated by calculating the *Mean* and *Standard Deviation (STD)* of all branches' power flow (pf) and the line percentage of MVA limit

(p%). Table 5 shows the network properties for all network structure and the corresponding optimal power flow, showing that the optimized networks have better network properties than their original counterparts.

All the R_{ECO} optimized networks have higher R_{CF} , showing that the ecological robustness corresponds to an improved robustness to cascading failures. Increasing R_{CF} is found to highly correlate with increasing

R_{ECO} , except in the optimized results of the IEEE 24 Bus RTS and the ACTIVSg500 case with 100 candidate branches. The optimized network structures in both these cases have a slightly higher value of R_{ECO} than the corresponding network with optimal power flow but lower R_{CF} s. One interesting observation is made for the ACTIVSg500-200-OPF: since the optimized network doesn't add any branches but only redistribute the power flows to achieve a higher R_{ECO} , the corresponding R_{CF} is also increased. R_{ECO} and R_{CF} of the optimal power flow are both higher than in the ACTIVSg500-50-Structure, ACTIVSg500-50-OPF, ACTIVSg500-100-Structure and ACTIVSg500-100-OPF.

All the R_{ECO} optimized networks have larger \bar{d} and \bar{c} , and reduced \bar{b} and \bar{l} . The ACTIVSg200 and ACTIVSg500 are synthetic grids, whose complex network properties are very close to actual grids. For actual networks, the \bar{d} is in the range of (2.58, 2.61), the \bar{c} is in the range of (0.032, 0.058), the \bar{b} is in the range of (0.083, 0.40), and the \bar{l} is in the range of (14.2, 29.2). The results show that the optimized networks' \bar{d} and \bar{c} are close to the actual systems, but the \bar{b} and \bar{l} are not. These can be explained by the way candidate branches were selected at their highest voltage level for each case, whose shortest distance is smaller than branches between different voltage levels.

The *Mean* and *Standard Deviation (STD)* of all the branches' power flow (pf) and line percentage of MVA limits (p%) clearly show that the R_{ECO} optimized networks distribute their power flow more equally than the original network. The Mean (pf) and STD (pf) in each optimized network with optimal power flow are smaller than the network with original generator set-points, showing that the network with optimal power flows distribute real power more equally. However, for the Mean(p%) and STD(p%), the network with optimal power flow has higher values than the corresponding network structure, so the network distributes the whole power (real and reactive power) less equally (still better than the original network). This is because the proposed MINLP problem is only solved with the DC power flow model (consider only the real power).

6.2. Network Reliability Comparison

$N-1$, $N-2$ and $N-3$ contingency analyses are done for the IEEE 24 Bus RTS cases to see whether the ecological robustness oriented networks perform better during the disturbances. A comprehensive $N-2$ and $N-3$ contingency analysis is difficult to complete for the ACTIVSg200 and ACTIVSg500 cases due to the number of network components and instead an $N-1$ contingency

analysis is done for the branch and substations respectively. The loss of one substation can catastrophically impact the entire system, providing a good validation of the redesigned system's ability to absorb large disturbances. Additionally, Narimani *et al.* and Huang *et al.* have utilized Line Outage Distribution Factors (LODFs) and Group Betweenness Centrality (GBC) to successfully identify sets of critical elements in synthetic grids, whose out of service can cause the system under stress [44, 45]. All the contingency analyses investigated here are performed without remedial actions. Original functionalities, such as automatic generation control (AGC) and automatic voltage regulator (AVR), are retained at their original settings enabling the proposed MINLP problem to be evaluated for its ability to improve the grid's ability to absorb unexpected emergencies by strategically expanding the network.

Table 6 shows the $N-1$, $N-2$ and $N-3$ contingency analysis for all the IEEE 24 Bus RTS cases. Under the $N-1$ contingency analysis, the IEEE 24 Bus RTS-50-Structure and -150-Structure cases have less violations than the original network. The IEEE 24 Bus RTS-50-OPF, -100-Structure and -200-Structure have more violations. As to $N-2$ contingency analysis, except the IEEE 24 Bus RTS-50-OPF case and -100-Structure case, the other cases have less violations. All the optimized networks have no unsolved situations to ensure the system is observable to operators when contingencies happen. The optimized networks have far fewer unsolved situations than the original network for the $N-3$ contingency analysis, reduced from 148 to less than 20. The IEEE 24 Bus RTS-150-Structure, -200-Structure and -200-OPF have fewer violations than the original network. The IEEE 24 Bus RTS-150-Structure has the best reliability, improving in all the tested $N-x$ contingency analyses. When considering the total number of $N-x$ contingencies, the normalized number violations (violations/total number of contingencies) are reduced for all the cases as well, as shown in Table 7.

Table 8 shows the contingency analysis for all ACTIVSg200 cases. All the optimized ACTIVSg200 cases maintain the same $N-1$ reliability as the original network. With the $N-1$ Substation contingency, all the optimized networks are *more* reliable with fewer violations and unsolved situations. With the critical contingencies from [44, 45], all the optimized networks are found to be more reliable than in their original form. ACTIVSg200-200-OPF has the best performance out of all the optimized network. Compared with the IEEE 24 Bus RTS case, the original ACTIVSg200 has more generation capacity meaning that even with 51 new branches added in this case, the generators are better able to support the

Table 5: Network properties for all variations of the IEEE 24 Bus, ACTIVSg200, and ACTIVSg500 case studies.

Use Case	Achieved R_{ECO}	R_{CF} [43]	\bar{d}	\bar{c}	\bar{b}	\bar{l}	Mean(pf)	STD(pf)	Mean(p%)	STD(p%)
IEEE 24 Bus RTS	0.3362	1.2517	2.833	0.03472	0.10063	3.2138	117.19	86.74	32.36	19.29
IEEE 24 Bus RTS-50-Structure	0.3485	4.0816	4	0.17698	0.07246	2.5942	67.01	53.33	10.44	5.30
IEEE 24 Bus RTS-50-OPF	0.3491	4.7299	4	0.17698	0.07246	2.5942	62.95	51.00	18.93	16.24
IEEE 24 Bus RTS-100-Structure	0.3509	5.1994	4.333	0.175	0.06637	2.4601	56.34	43.71	7.93	4.16
IEEE 24 Bus RTS-100-OPF	0.3498	6.2246	4.333	0.175	0.06637	2.4601	51.47	42.57	13.03	8.91
IEEE 24 Bus RTS-150-Structure	0.3446	4.0166	3.5	0.09861	0.08037	2.7681	69.68	60.11	21.24	18.41
IEEE 24 Bus RTS-150-OPF	0.3455	4.1494	3.5	0.09861	0.08037	2.7681	68.54	57.76	21.13	18.29
IEEE 24 Bus RTS-200-Structure	0.3464	2.2230	3.417	0.11389	0.07790	2.7138	97.94	60.66	21.46	8.96
IEEE 24 Bus RTS-200-OPF	0.3473	2.3714	3.417	0.11389	0.07790	2.7138	88.78	52.59	25.14	15.89
ACTIVSg200	0.2450	1.8815	2.46	0.03723	0.03531	7.9913	37.54	56.65	13.92	19.10
ACTIVSg200-50-Structure	0.2643	3.2543	2.65	0.04399	0.02899	6.7396	34.00	51.06	7.63	9.53
ACTIVSg200-50-OPF	0.2650	3.2837	2.65	0.04399	0.02899	6.7396	33.18	50.61	12.22	17.33
ACTIVSg200-100-Structure	0.2590	2.7135	2.55	0.03751	0.03061	7.0597	35.54	54.36	9.38	11.80
ACTIVSg200-100-OPF	0.2591	2.7134	2.55	0.03751	0.03061	7.0597	35.54	54.36	12.55	16.88
ACTIVSg200-150-Structure	0.2548	1.9877	2.51	0.03654	0.03145	7.2272	37.48	58.73	11.45	14.86
ACTIVSg200-150-OPF	0.2548	1.9877	2.51	0.03654	0.03145	7.2272	37.48	58.73	12.70	16.97
ACTIVSg200-200-Structure	0.2701	5.4204	2.82	0.05346	0.02787	6.5181	30.50	48.63	5.09	6.23
ACTIVSg200-200-OPF	0.2702	5.4205	2.82	0.05346	0.02787	6.5181	30.50	48.63	11.55	16.38
ACTIVSg500	0.2132	2.7952	2.344	0.01742	0.01668	9.3043	52.36	77.23	15.97	17.75
ACTIVSg500-50-Structure	0.2198	3.0058	2.352	0.01722	0.01647	9.2035	48.70	65.08	15.20	17.12
ACTIVSg500-50-OPF	0.2198	3.0046	2.352	0.01722	0.01647	9.2035	48.70	65.08	15.20	17.13
ACTIVSg500-100-Structure	0.2149	2.7313	2.348	0.01708	0.01615	9.0438	52.49	75.93	15.92	17.70
ACTIVSg500-100-OPF	0.2214	3.0606	2.348	0.01708	0.01615	9.0438	47.37	69.13	15.48	17.00
ACTIVSg500-150-Structure	0.2228	3.4439	2.404	0.01848	0.01409	8.0169	50.93	69.35	15.14	17.00
ACTIVSg500-150-OPF	0.2227	3.4343	2.404	0.01848	0.01409	8.0169	50.88	68.7	15.13	17.10
ACTIVSg500-200-OPF	0.2220	3.3624	2.344	0.01742	0.01668	9.3043	46.16	61.05	15.30	17.15

new network design.

Table 9 shows the contingency analysis for all the ACTIVSg500 cases. The $N-I$ contingency analysis (Branch) shows that the optimized networks do not improve much in regards to the number of violations in the system. However, for all cases, the extra violations come from voltage instability, which is associated with the reactive power support from the system. If the system doesn't have enough reactive power support in the system, with the extra transmission lines built, the system will experience more stress because of reactive power insufficiency. The $N-I$ contingency analysis (Substation) shows that the ACTIVSg500-100-OPF and ACTIVSg500-150-OPF cases both improve the number of contingencies as compared to the original network. The critical contingency analysis shows that the ACTIVSg500-50-Structure, -50-OPF, -100-OPF and -200-OPF cases are all more reliable than the original

network, resulting in a reduced number of violations and no unsolved situations. The ACTIVSg500-200-OPF stands out as a special grid case study in the analysis. The R_{ECO} optimized version of the network improves the grid's reliability during the tested critical contingencies without adding any new branches. This highlights the potential of R_{ECO} to guide the distribution of power flows to survive contingencies.

Even though the improvement for the ACTIVSg500 case is not as dramatic as is seen for the ACTIVSg200 case, the results show that with more real and reactive power support the R_{ECO} optimization can improve the network's performance.

6.3. Cost-Effective Analysis

Since the candidate branches are created through Algorithm 2, no cost information has been included with

Table 6: Reliability Comparison of Ecological Robustness Oriented Power Network (IEEE 24 Bus RTS)

Use Case	Achieved R_{ECO}	Number of Built Branches	$N-1$ Contingency	$N-2$ Contingency	$N-3$ Contingency
IEEE 24 Bus RTS	0.3362	0	4 violations	254 violations, 3 unsolved	6627 violations, 148 unsolved
IEEE 24 Bus RTS-50-Structure	0.3485	21	3 violation	208 violation	6808 violations, 11 unsolved
IEEE 24 Bus RTS-50-OPF	0.3491	21	7 violation	388 violation	10908 violations, 14 unsolved
IEEE 24 Bus RTS-100-Structure	0.3509	25	6 violation	351 violation	10268 violations, 11 unsolved
IEEE 24 Bus RTS-100-OPF	0.3498	25	4 violation	250 violation	7893 violations, 6 unsolved
IEEE 24 Bus RTS-150-Structure	0.3446	12	3 violation	203 violation	6206 violations, 16 unsolved
IEEE 24 Bus RTS-150-OPF	0.3455	12	4 violation	242 violation	7020 violations, 17 unsolved
IEEE 24 Bus RTS-200-Structure	0.3464	8	4 violation	166 violation	4366 violations, 12 unsolved
IEEE 24 Bus RTS-200-OPF	0.3473	8	5 violation	238 violation	5695 violations, 15 unsolved

respect to their constructing. The cost analysis here assumes the costs of all branches in all cases are the same.

The most cost-effective network design and system operation for the IEEE 24 Bus RTS case is the IEEE 24 Bus RTS-200-Structure. This was also the best performing design (unsolved situations were reduced from 3 and 148, to 0 and 12, for the $N-2$ and $N-3$ contingencies respectively), suggesting that the biological behavior described by maximizing R_{ECO} is able to minimize both violations AND cost. The ACTIVSg200-150-Structure is the most cost-effective network design for the ACTIVSg200 case. Despite having more violations and unsolved situations than other optimized networks, it only adds five branches to maximize R_{ECO} . The ACTIVSg500-100-OPF network design and operating point is the best performing design under contingencies, with only one more branch built and adjusted generator setpoints.

The proposed MINLP is only solved in the DC power flow model, which doesn't consider the reactive power in the system. The network design and expansion in practice should consider the corresponding support of

real and reactive power. Added reactive power reserves would further improve the effectiveness of these networks. Moreover, investments in network architecture also contribute to supporting load increases in the future. A more detailed analysis of the cost-effectiveness of these biologically inspired network designs is needed to consider the impact of increased loads, generation, and a system's power transfer capability. More realistic data for candidate branches, including construction costs and benefits, would further validate the cost-effectiveness of ecological robustness as a guide for power grid network design.

7. Discussion

Ecological robustness (R_{ECO}) quantifies the balance between pathway efficiency and redundancy in biological food webs. The unique range of R_{ECO} that has been found for food webs, known as the "window of vitality," has been hypothesized by ecologists to be the result of their ability to both survive disturbances while simultaneously growing and developing [23, 28, 22]. Modeling

Table 7: Normalized Violations of Ecological Robustness Oriented Power Network (IEEE 24 Bus RTS)

Use Case	Achieved R_{ECO}	Number of Built Branches	$N-1$ Contingency	$N-2$ Contingency	$N-3$ Contingency
IEEE 24 Bus RTS	0.3362	0	0.1053	0.3613	0.7856
IEEE 24 Bus RTS-50-Structure	0.3485	21	0.0508	0.1776	0.2094
IEEE 24 Bus RTS-50-OPF	0.3491	21	0.1186	0.3313	0.3355
IEEE 24 Bus RTS-100-Structure	0.3509	25	0.0952	0.1797	0.2586
IEEE 24 Bus RTS-100-OPF	0.3498	25	0.0635	0.1280	0.1987
IEEE 24 Bus RTS-150-Structure	0.3446	12	0.0600	0.1657	0.3166
IEEE 24 Bus RTS-150-OPF	0.3455	12	0.0800	0.1976	0.3581
IEEE 24 Bus RTS-200-Structure	0.3464	8	0.0870	0.1603	0.2876
IEEE 24 Bus RTS-200-OPF	0.3473	8	0.1087	0.2230	0.3752

power systems as a food web directional graph, where the nodes represent critical network actors and the edges the flow of materials/energy between them, enables the application of R_{ECO} and the Window of Vitality to the design of power grids. The method used here populates the Ecological Flow Matrix with the grid's real power flows, setting up the maximization of R_{ECO} to guide power network design. Prior work was only able to show the success of this method for small grid test cases. The relaxation of R_{ECO} proposed here, along with the incorporation of power system constraints, formulates a solvable MINLP problem for larger and more realistic power grid networks. The analysis of both network properties and reliability supports the use of this biological characteristic as a novel method to improve grid robustness and highlights additional improvements including better network properties, more equally distributed power flow over the system, and improved reliability against unexpected contingencies.

The maximum value of R_{ECO} is 0.3679 ($1/e$), with the original ecological formulation of R_{ECO} following Equations (1)-(4). The proposed relaxation shifts this maximum value to 0.3431 and enables its use for large

power system networks when coupled with the DC power flow model. The difference between the original maximum of 0.3679 and the relaxed maximum of 0.3431 is acceptable considering only a first order Taylor Series Expansion is used.

After constructing the new branches from the candidate branches, the achieved R_{ECO} in each network are different from the solved optimal value. The value of achieved R_{ECO} for IEEE 24 Bus RTS optimized networks are higher than the solved R_{ECO} . Besides, the achieved R_{ECO} of IEEE 24 Bus RTS-200-Structure is higher than IEEE 24 Bus RTS-150-Structure with less branches built. Under different candidate branch sets, it shows that the R_{ECO} is strategically designing the network structure to achieve an optimal R_{ECO} by selecting the satisfying branches from candidate branches. For the synthetic cases, the value of achieved R_{ECO} is much less than the solved optimal R_{ECO} . The original synthetic power grids are highly close to the real U.S power grids, which are quite sparse and efficient. The candidate branches for those cases are focused on the high voltage branches and they are a small portion of all potential branches in the system. Since R_{ECO} evaluates the

Table 8: Reliability Comparison of Ecological Robustness Oriented Power Network (ACTIVSg200)

Use Case	Achieved R_{ECO}	Number of Built Branches	$N-1$ Contingency (Branch)	$N-1$ Contingency (Substation)	Critical Contingency [44, 45]
ACTIVSg200	0.2450	0	0	5 violations, 2 unsolved	1030 violations, 17 unsolved
ACTIVSg200-50-Structure	0.2643	26	0	1 violation	29 violations, 2 unsolved
ACTIVSg200-50-OPF	0.2650	26	0	1 violation	29 violations, 2 unsolved
ACTIVSg200-100-Structure	0.2590	15	0	1 violation, 1 unsolved	53 violations, 2 unsolved
ACTIVSg200-100-OPF	0.2591	15	0	1 violation, 1 unsolved	52 violations, 2 unsolved
ACTIVSg200-150-Structure	0.2548	5	0	3 violation, 1 unsolved	352 violations, 3 unsolved
ACTIVSg200-150-OPF	0.2548	5	0	3 violation, 1 unsolved	352 violations, 3 unsolved
ACTIVSg200-200-Structure	0.2701	51	0	1 violation	26 violations, 2 unsolved
ACTIVSg200-200-OPF	0.2702	51	0	1 violation	16 violations

power flow path efficiency and redundancy, with only a few redundancy being added, the achieved R_{ECO} won't be as high as the optimal R_{ECO} . However, with the added branches from the solved MINLP problem, there are improvement of R_{ECO} , network properties, and system's ability of absorbing disturbances and changes.

As shown in Section 6, the optimized network properties are overall better than the original network, which shows the improvement of the system's robustness. With another entropy based robustness metric R_{CF} [43], the trend between R_{ECO} and R_{CF} is highly correlated with the optimized network and power flow, which is not entirely surprising as both metrics consider both the network topology and power flow in the system. The trend is more interesting when one considers that R_{CF} only focuses on the grid's robustness, as defined by its electrical nodal robustness and node significance, while R_{ECO} considers the efficiency and redundancy of power flow pathways in the network. The comparison of the distribution of real power flow and branches' MVA percentage (p%), the optimized network structure with the

optimal power flow settings distribute the real power more equally over the network for all branches, but they do not distribute the real and reactive power more equally with the consideration of branch MVA limits. Since the candidate branches created through Algorithm 2 utilizes the existing branches' physical information with normal distribution, their physical parameters are correlated with existing branches. Thus, the less equally distributed real and reactive power flow is because of the re-distributed reactive power, which is not captured in the formulation of EFM and the MINLP is not solved with AC power flow model. For the reliability analysis, there are improvements from the optimized network, especially the optimized ACTIVSg200 cases. All of them have better reliability than the original network and the improvements are significant. With the data of online real and reactive power capacity and loading for each case, the ACTIVSg200 has the most reserves for extra branches, which ensures the optimized networks can maintain both real and reactive consumption and the reliability during contingency. Even though the IEEE 24

Table 9: Reliability Comparison of Ecological Robustness Oriented Power Network (ACTIVSg500)

Use Case	Achieved R_{ECO}	Number of Built Branches	$N-1$ Contingency (Branch)	$N-1$ Contingency (Substation)	Critical Contingency [44, 45]
ACTIVSg500	0.2132	0	38 violations	66 violations	52 violations, 8 unsolved
ACTIVSg500-50-Structure	0.2198	2	41 violations	70 violation	46 violations
ACTIVSg500-50-OPF	0.2198	2	41 violations	70 violation	46 violations
ACTIVSg500-100-Structure	0.2149	1	38 violations	69 violation	40 violations, 8 unsolved
ACTIVSg500-100-OPF	0.2214	1	39 violations	65 violation	42 violations
ACTIVSg500-150-Structure	0.2228	14	41 violations	70 violation	53 violations, 8 unsolved
ACTIVSg500-150-OPF	0.2227	14	40 violations	58 violation	60 violations, 8 unsolved
ACTIVSg500-200-OPF	0.2220	0	39 violations	66 violation	41 violations

Bus RTS and ACTIVSg500 do not have that much reserve compared to ACTIVSg200, there are still some optimized networks have better reliability than the original network. This observation shows the effectiveness of using R_{ECO} as a guidance to design and expand power grid network to improve its ability of absorbing sudden and big disturbances in the system with better reliability. It also emphasizes the importance of considering reactive consumption and compensation for power network expansion.

8. Conclusion and Future Work

This paper presents a bio-inspired method for re-designing power grid networks to improve resilience. The work reformulates an optimization solution for larger scale grids with a mixed-integer nonlinear programming (MINLP) problem while maintaining the objective of mimicking food web levels of the ecological robustness R_{ECO} metric for power systems. Due to R_{ECO} 's complexity, a Taylor Series Expansion is used to relax its formulation. The relaxed MINLP problem is applied to four power system cases solved using DC

power flow models. The analysis shows that the biologically optimized networks have improved network properties and increased reliability under critical contingencies. The optimized networks are better able to absorb both sudden changes and big disturbances without remedial actions. The results show that the proposed MINLP problem can improve power systems' resilience by strategically constructing networks under the guidance of ecological robustness.

Future work is needed to address three areas highlighted for improvement. First, additional relaxation schemes may need to be investigated for the proposed MINLP problem to be solved using an AC power flow model and consider reactive power consumption in new network structures. Second, additional details should be added into the cost calculations of new branches to better understand the economics of the bio-inspired designs. This may include information about location, distance, time, critical loads, and benefits not only in terms of fewer contingencies but also added power transfer capabilities. Third, additional ways to use ecological robustness should be investigated, including for power systems operation for redundancy and efficiency and for

power flow dispatch against disturbances.

Acknowledgment

The authors would like to acknowledge the US Department of Energy Cybersecurity for Energy Delivery Systems program under award DE-OE0000895, the National Science Foundation under Grant 1916142, and the Texas A&M Energy Institute for their support of this project.

References

- [1] Y. Wang, C. Chen, J. Wang, R. Baldick, Research on resilience of power systems under natural disasters? a review, *IEEE Transactions on Power Systems* 31 (2) (2015) 1604–1613.
- [2] H. Haes Alhelou, M. E. Hamedani-Golshan, T. C. Njenda, P. Siano, A survey on power system blackout and cascading events: Research motivations and challenges, *Energies* 12 (4) (2019) 682.
- [3] S. A. Shield, S. M. Quiring, J. V. Pino, K. Buckstaff, Major impacts of weather events on the electrical power delivery system in the united states, *Energy* 218 (2021) 119434.
- [4] E. Targett, High Voltage Attack: EU's Power Grid Organisation Hit by Hackers (March 2020).
URL <https://www.cbronline.com/news/eu-power-grid-organisation-hacked>
- [5] Defense Use Case, Analysis of the cyber attack on the ukrainian power grid, Electricity Information Sharing and Analysis Center (E-ISAC) (2016).
- [6] L. Das, S. Munikoti, B. Natarajan, B. Srinivasan, Measuring smart grid resilience: Methods, challenges and opportunities, *Renewable and Sustainable Energy Reviews* 130 (2020) 109918.
- [7] H. Chen, F. S. Bresler III, M. E. Bryson, K. Seiler, J. Monken, Toward bulk power system resilience: approaches for regional transmission operators, *IEEE Power and Energy Magazine* 18 (4) (2020) 20–30.
- [8] R. Moreno, M. Panteli, P. Mancarella, H. Rudnick, T. Lajos, A. Navarro, F. Ordóñez, J. C. Araneda, From reliability to resilience: Planning the grid against the extremes, *IEEE Power and Energy Magazine* 18 (4) (2020) 41–53.
- [9] A. Gholami, T. Shekari, M. H. Amirioun, F. Aminifar, M. H. Amini, A. Sargolzaei, Toward a consensus on the definition and taxonomy of power system resilience, *IEEE Access* 6 (2018) 32035–32053.
- [10] M. Ouyang, L. Duenas-Orsorio, Multi-dimensional hurricane resilience assessment of electric power systems, *Structural Safety* 48 (2014) 15–24.
- [11] M. Panteli, P. Mancarella, D. N. Trakas, E. Kyriakides, N. D. Hatziaargyriou, Metrics and quantification of operational and infrastructure resilience in power systems, *IEEE Transactions on Power Systems* 32 (6) (2017) 4732–4742.
- [12] M. Panteli, P. Mancarella, Modeling and evaluating the resilience of critical electrical power infrastructure to extreme weather events, *IEEE Systems Journal* 11 (3) (2015) 1733–1742.
- [13] B. Cai, M. Xie, Y. Liu, Y. Liu, Q. Feng, Availability-based engineering resilience metric and its corresponding evaluation methodology, *Reliability Engineering and System Safety* 172 (2018) 216–224.
- [14] T. Dave, A. Layton, Designing ecologically-inspired robustness into a water distribution network, *Journal of Cleaner Production* 254 (2020) 120057. doi:10.1016/j.jclepro.2020.120057.
- [15] A. Chatterjee, A. Layton, Bio-inspired design for sustainable and resilient supply chains, *Procedia CIRP* 90 (2020) 695–699. doi:10.1016/j.procir.2020.01.127.
- [16] A. Chatterjee, A. Layton, Mimicking nature for resilient resource and infrastructure network design, *Reliability Engineering and System Safety* 204 (2020) 107142.
- [17] A. Layton, B. Bras, M. Weissburg, Ecological robustness as a design principle for sustainable industrial systems, in: *International Design Engineering Technical Conferences and Computers and Information in Engineering Conference*, p. V004T05A047. doi:10.1115/DETC2015-47560.
- [18] A. Chatterjee, R. Malak, A. Layton, Exploring a bio-inspired system of systems resilience vs. affordability tradespace, *Journal of Computing and Information Science in Engineering* (2021). doi:10.1115/1.4050288.
- [19] A. Chatterjee, R. Malak, A. Layton, A bio-inspired framework for analyzing and predicting the trade-off between system of systems attributes, in: *Conference on Systems Engineering Research*, 2020.
- [20] V. Panyam, H. Huang, B. Pinte, K. Davis, A. Layton, Bio-inspired design for robust power networks, in: *2019 IEEE Texas Power and Energy Conference (TPEC)*, IEEE, 2019, pp. 1–6.
- [21] V. Panyam, H. Huang, K. Davis, A. Layton, Bio-inspired design for robust power grid networks, *Applied Energy* 251 (2019) 113349.
- [22] R. E. Ulanowicz, S. J. Goerner, B. Lietaer, R. Gomez, Quantifying sustainability: resilience, efficiency and the return of information theory, *Ecological complexity* 6 (1) (2009) 27–36.
- [23] R. E. Ulanowicz, Quantitative methods for ecological network analysis, *Computational Biology and Chemistry* 28 (5) (2004) 321–339. doi:10.1016/j.compbiolchem.2004.09.001.
- [24] H. Huang, V. Panyam, M. R. Narimani, A. Layton, K. R. Davis, Mixed-integer optimization for bio-inspired robust power network design, in: *52nd North American Power Symposium*, 2021.
- [25] C. Coffrin, R. Bent, K. Sundar, Y. Ng, M. Lubin, Powermodels.jl: An open-source framework for exploring power flow formulations, in: *2018 Power Systems Computation Conference (PSCC)*, IEEE, 2018, pp. 1–8.
- [26] R. E. Ulanowicz, J. S. Norden, Symmetrical overhead in flow networks, *International Journal of Systems Science* 21 (2) (1990) 429–437.
- [27] R. E. Ulanowicz, An Hypothesis on the Development of Natural Communities, *J. theor. Biol* 85 (1980) 223–245.
- [28] R. E. Ulanowicz, *Growth and Development: Ecological Phenomenology*, 1st Edition, Springer-Verlag, New York, 1986. doi:10.1007/978-1-4612-4916-0.
- [29] A. Layton, Food webs: realizing biological inspirations for sustainable industrial resource networks, Ph.D. thesis, Georgia Institute of Technology (2014).
- [30] The north american electric reliability corporation (nerc) (mar 2006).
URL <https://www.nerc.com/Pages/default.aspx>
- [31] R. D. Zimmerman, C. E. Murillo-Sánchez, *Matpower 6.0 user's manual*, Power Systems Engineering Research Center 9 (2016).
- [32] A. B. Birchfield, T. Xu, K. M. Gegner, K. S. Shetye, T. J. Overbye, Grid structural characteristics as validation criteria for synthetic networks, *IEEE Transactions on Power Systems* 32 (4) (2017) 3258–3265. doi:10.1109/TPWRS.2016.2616385.
- [33] G. Casella, R. L. Berger, *Statistical inference*, Cengage Learning, 2021.
- [34] V. Panyam, A. Layton, Bio-inspired modeling approaches for

- human networks with link dissipation, ASME 2019 International Design Engineering Technical Conferences and Computers and Information in Engineering Conference (August 18-21 2019). doi:10.1115/DETC2019-98171.
- [35] J. Duncan Glover, M. Sarma, T. Overbye, Power System Analysis and Design, 5th Edition, Cengage Learning, 2012.
 - [36] P. Belotti, C. Kirches, S. Leyffer, J. Linderoth, J. Luedtke, A. Mahajan, Mixed-integer nonlinear optimization, *Acta Numerica* 22 (2013) 1–131.
 - [37] A. Wächter, L. T. Biegler, On the implementation of an interior-point filter line-search algorithm for large-scale nonlinear programming, *Mathematical programming* 106 (1) (2006) 25–57.
 - [38] O. Kröger, C. Coffrin, H. Hijazi, H. Nagarajan, Juniper: An open-source nonlinear branch-and-bound solver in julia, in: *International Conference on the Integration of Constraint Programming, Artificial Intelligence, and Operations Research*, Springer, 2018, pp. 377–386.
 - [39] F. John, V. Stefan, R. Ted, G. S. Haroldo, F. Dan, H. Lou, H. Bill, K. Bjarni, P. Cindy, S. Edwin, L. Miles, W. Jean-Paul, S. Matthew, Cbc (coin-or branch and cut) open-source mixed integer programming solver (jun 2019).
URL <https://github.com/coin-or/Cbc>
 - [40] Z. Jin, G. Jin, *Mathematical analysis*, Dalian University of Technology Press Dalian, 2007.
 - [41] PowerWorld Corporation, available at <http://www.powerworld.com>, 2018.
 - [42] B. L. Thayer, Z. Mao, Y. Liu, K. Davis, T. Overbye, Easy simauto (esa): A python package that simplifies interacting with powerworld simulator, *Journal of Open Source Software* 5 (50) (2020) 2289. doi:10.21105/joss.02289.
 - [43] Y. Koç, M. Warnier, R. E. Kooij, F. M. Brazier, An entropy-based metric to quantify the robustness of power grids against cascading failures, *Safety science* 59 (2013) 126–134.
 - [44] M. R. Narimani, H. Huang, A. Ummunnakwe, Z. Mao, A. Sahu, S. Zonouz, K. Davis, Generalized contingency analysis based on graph theory and line outage distribution factor, *arXiv preprint arXiv:2007.07009* (2020).
 - [45] H. Huang, Z. Mao, M. R. Narimani, K. R. Davis, Toward efficient wide-area identification of multiple element contingencies in power systems, in: *2021 IEEE Power and Energy Society Innovative Smart Grid Technologies Conference (ISGT)*, IEEE, 2021, pp. 01–05.